Effect of Seat and Seat Belt characteristics on the Lumbar Spine and Pelvis Loading of the SAFER Human Body Model in reclined Postures

Krystoffer Mroz, Martin Östling, Rachel Richardson, Jason Kerrigan, Jason Forman, Bronislaw Gepner, Nils Lubbe, Bengt Pipkorn

Abstract Load limiters at seat track, seat, seat back, and lap belt were investigated to determine their effect on pelvis and lumbar spine loading, using the SAFER human body model and models of a semi-rigid seat and a triple-pretensioned, load-limited belt system. The models were evaluated with four sled tests involving 50 km/h frontal impacts using average-size male post-mortem human subjects reclined at 50 deg. Modelled results for excursions of the head, T1, T8, T11, L1, L3, and pelvis – together with pelvis rotations and belt forces – correlated well with the sled test results, with a total correlation and analysis rating of 0.81. The largest reduction in lumbar spine loading was obtained from seat track and seat load limiting, while the largest reduction in pelvis loading was obtained from seat track and double lap belt load limiting. Seat back load limiting led to only a small reduction of pelvis and lumbar spine loading. The combined effect of seat track, seat, and lap belt load limiting reduced L1-L2 lumbar spine compression forces from 4 to 2 kN, flexion moments from 100 to 42 Nm, and total pelvis anterior superior iliac spine forces from 9.1 to 4.5 kN.

Keywords Lumbar spine, pelvis, reclined, SAFER HBM, seat belt

I. INTRODUCTION

Future autonomous driving vehicles are expected to offer new vehicle interiors and seating configurations, such as rotating seats that permit relaxing, socialising, and working [1], because the occupant no longer needs to constantly interact with the control systems of the vehicle. In fact, the occupant will be able to move away from the frontal restraint systems such as airbag, knee bolster, and knee airbag – as well as the footwell. Occupants are also expected to relax in postures which are more reclined than current upright driving postures [2,3].

In more reclined seated postures, the pelvis angle is rotated more rearward. The occupant is more likely to submarine, the process in which the lap belt slides over the anterior superior iliac spine (ASIS) of the pelvic bone and penetrates the abdominal area in case of an impact. Hollow-organ injuries of the abdomen and, potentially, lumbar spine injuries have been identified as a result [4].

As overall vehicle safety has improved over the years, lumbar spine injuries have not decreased to the same degree as some other injury types [5-7]. Newer cars are structurally stiffer to avoid intrusions, which has made them safer but increases the relative risk of lumbar spine injuries [8,9]. Furthermore, human body simulations have shown that reclined occupants experience more loading to the lumbar spine than upright occupants [10]. Further, several studies have reported pelvis fractures from belt loading in post-mortem human subjects (PMHS) experiencing frontal impact loading. Pelvis fractures were obtained in the iliac wings of an upright PMHS seated in rigid [11] and vehicle seats [12]. Pelvis iliac crest fractures were obtained for PMHS in slouched positions in a semi-rigid seat [13]. Using a semi-rigid seat in a softer configuration, which promotes larger pelvis excursions, pelvis iliac wing fractures were still obtained [14]. These studies indicate the importance of seat stiffness for the loading of the pelvis and, to a lesser extent, the lumbar spine.

The SAFER human body model (HBM) is a mathematical model of an adult mid-sized male which was developed to improve the understanding of impact response and injury mechanisms in humans. The SAFER HBM, originally developed from Total Human Model for Safety (THUMS) version 3 [15], has been updated with

K. Mroz (krystoffer.mroz@autoliv.com; tel: +46733614346) and M. Östling are Research Specialists, N. Lübbe, Director Research and B. Pipkorn, Director Simulation Active Structures, at Autoliv Research, Vårgårda, Sweden. R. Richardson, Ph.D. Student, J. Kerrigan, Director, J. Forman, Principal Scientist and B. Gepner, Research Scientist, are at the Center for Applied Biomechanics, University of Virginia, USA.

new head, neck, and rib cage models [16]. The lumbar spine was also modified, with updated geometric modelling of the vertebrae and the material properties of the intervertebral ligaments and discs, as well as new contact definitions to improve the biofidelity [17,18]. The capability of the HBM model to predict kinematics and rib fractures has been evaluated at both the component and whole body levels [19], although the latter were limited to upright seated postures. Differences between the SAFER HBM and other HBMs in pelvis and lumbar spine kinematics and loading, as well as submarining, for a reclined posture were reported in [20]. However, at the time there were no kinematic reference data available to evaluate the HBMs.

In this study, the first objective was to evaluate the SAFER human body model with respect to whole body, pelvis and lumbar spine kinematics in a reclined posture by means of sled tests using reclined average male PMHS in frontal impacts. The second objective was to use the evaluated model to quantify the effects of seat track, seat, seat back, and lap belt load limiting on the reduction of loading on the pelvis and lumbar spine.

II. METHODS

The study was carried out for a belted, passenger side, reclined occupant in a generic environment consisting of a semi-rigid seat [14] and a seat-integrated, triple-pretensioned, load-limited three-point belt system with a crash locking tongue [21]. A footwell was used for the model evaluation but not in the parameter study. The mathematical simulations were performed using the finite element (FE) program LS-DYNA version 971 R9.3.1 [22] and the statistical evaluations using Minitab version 17 [23].

Human Body Model Evaluation to Reclined PMHS Tests

An FE model of the physical generic environment used in reclined PMHS tests [21] was developed. The FE models of the seat, seat belt and the SAFER HBM Version 9.0.1 were evaluated by means of four sled tests in 50 km/h frontal impacts with reclined average male PMHS [21,24,25].

The FE model of the semi-rigid seat used in [14] was further developed for this study, Fig. 1. The model consists of two adjustable plates: the seat and submarining pans. Their geometry and stiffness response were configured to match a vehicle seat [14]. The modelling of the seat and submarining pan spring systems was updated, and the seat pan was shortened by 20 mm to avoid interaction with the submarining pan. The modified seat model was then validated by comparing moment-rotation responses under static loading against reference data for both front and rear-seat configurations in [14], see Appendix Fig. A1. In the PMHS tests, the front configuration used a 15.5 deg seat pan angle, 30 deg submarining pan angle, 128 N/mm seat pan side spring stiffness, 379 N/mm seat pan centre spring stiffness, and 132 N/mm submarining pan spring stiffness.

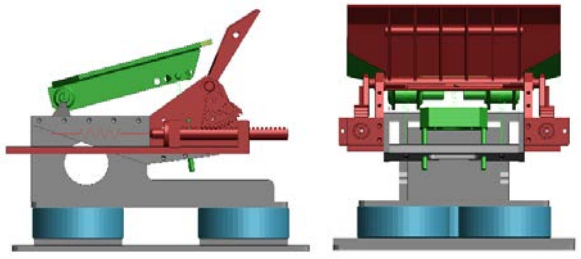

Fig. 1. Model of the semi-rigid seat (front seat configuration) with the seat pan in green and the submarining pan adjustable arrangement in red.

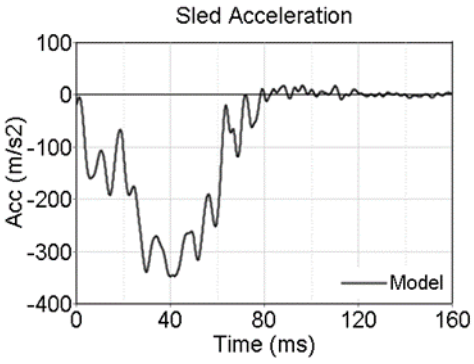

Fig. 2. Crash pulse 50 km/h.

A three-point seat belt system with a seatback-mounted D-ring was used to ensure that the shoulder belt geometry did not change for different seat back angles. The belt system was designed to improve pelvis restraint in order to avoid submarining [26]. To accomplish this, the belt system consisted of lap belt pretensioners at both the outboard anchor and inboard buckle points, together with a crash locking tongue that

mitigated webbing transfer from the shoulder belt to the lap belt. The shoulder belt was equipped with a retractor pretensioner and a load limiter of 3.5 kN [26]. Seatback deformation was not considered. The buckle lap pretensioner was activated at 3 ms and the remaining two pretensioners at 9 ms. Autoliv models of the pretensioners, retractors, and webbing material, which closely matched their mechanical counterparts, were used for the model of the belt system. The belt anchorage points and belt routing on the chest were defined from average 3D optoelectronic motion tracking and 3D position measurements of the PMHS test setup [21].

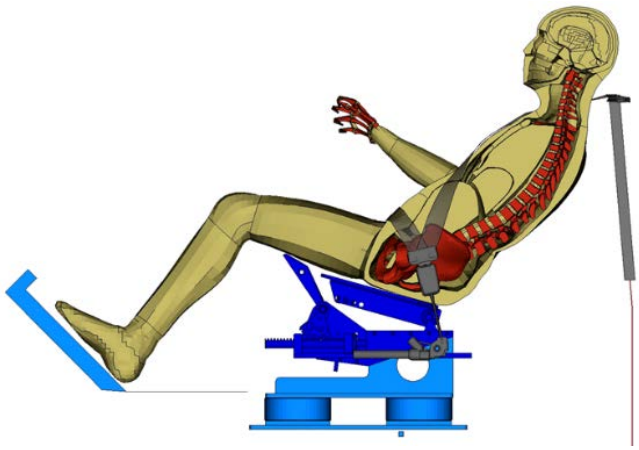

Fig. 3. Reclined SAFER HBM in the generic environment with the semi-rigid seat, the seat-integrated belt system and the footwell.

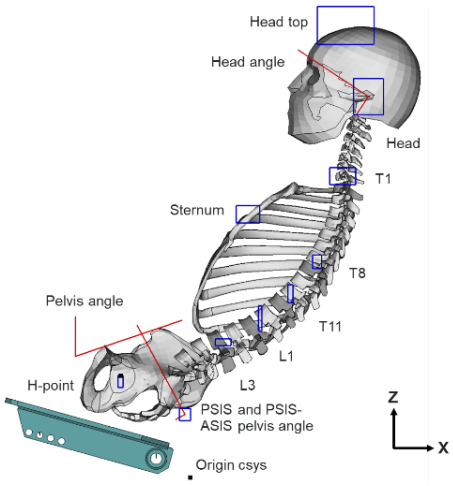

Fig. 4. Position of the reclined SAFER HBM compared to the target positioning corridors from 3D position measurements on the PMHS [27].

The SAFER HBM was positioned in an approximately 50 deg reclined posture as measured on the sternum with respect to the vertical (approximately 25 deg from a typical upright seated posture), using target positioning data from 3D position measurements on the PMHS, Fig. 3 and Fig. 4. From the PMHS measurements, standard deviation corridors were derived for head top, head, T1, T8, T11, L1, L3, PSIS and H-point, as well as pelvis and head angles [27]. The HBM was positioned by approximately matching the centre of each skeleton part to the derived positioning corridor, with a specific focus on the positions of the pelvis and lumbar spine. The HBM's initial pelvis angle was 72 deg as measured between ASIS and pubic symphysis to the vertical and the initial head angle 32 deg as measured between the zygomatic process and the eye orbit to the horizontal, both angles defined in the sagittal plane. The HBM's lumbar spine length was shorter than the PMHS average, but the thoracic spine length was similar.

The semi-rigid seat, seat belt, and SAFER HBM were subjected to a full-frontal, 50 km/h 35-g pulse. The crash pulse corresponded to the pulse used in several previous PMHS tests [14], Fig. 2. The excursions of the head, T1, T8, T11, L1, and pelvis, together with pelvis rotations and lap belt forces from the model, were compared to those of four sled tests with average male reclined PMHS aged 25-72 years old (Table I). PMHS 2 was excluded due to substantial mass difference relative to the other subjects and the SAFER HBM. Pelvis fracture was obtained at the right iliac wing between the ASIS and anterior inferior iliac spine (AIIS) for PMHS 1 and 3 [24]. PMHS 1 and 3 also sustained lumbar spine fractures at the L1 vertebra [25]. PMHS 5 submarined at the buckle side (left iliac wing).

The seat, seat belt and HBM model responses were assessed using the correlation and analysis (CORA) method [28], in which the total rating is calculated using two correlation metrics, cross-correlation and corridor. The cross-correlation metric quantifies the correlation of the phase, size, and shape of the model responses to those of the test. The corridor metric evaluates the degree of fit of the model responses to a corridor derived from the test responses. The CORA rating was derived using nine responses during the evaluation time window of 0 to 150 ms.

In this study, the SAFER HBM was modified by increasing the friction between the pelvis bone and the pelvis soft tissue from 0.2 to 0.6 to improve the correlation of the model's pelvis rotations with those of the PMHS tests.

TABLE I
ANTHROPOMETRY AND INJURIES FOR PMHS IN RECLINED FRONTAL SLED TESTS. PMHS NUMBERING ACC. TO [24,25].

PMHS No	Test No	Height (cm)	Weight (kg)	Age (years)	Pelvis fracture location	Lumbar spine fracture location
1	s0529	175	74.4	66	RHS between ASIS and AIIS	L1 compression
3	s0531	185	73.9	72	RHS between ASIS and AIIS	L1 burst
4	s0532	174	75.0	25	-	-
5	s0533	180	74.4	55	-	-

Full Factorial Parameter Study

The evaluated SAFER HBM model was then used in a two-level full factorial study with four factors, resulting in 16 simulations. The four factors were: seat track load limiting in frontal direction (SeatTrack_LLx), seat and submarining pan load limiting in vertical direction (Seat_LLz), seat back rotational load limiting (SeatBack_LL) and lap belt load limiting on both anchor and buckle sides (Lap_LL), Table II and Fig. 5.

TABLE II
FULL FACTORIAL PARAMETER STUDY – FACTORS AND LOAD LIMITING (LL) LEVELS

Factor	Low level (0)	High Level (1)
Seat track LL in frontal direction (SeatTrack_LLx)	None	21 kN
Seat and submarining pan LL in vertical direction (Seat_LLz)	None	8 kN
Lap belt LL, anchor and buckle sides (Lap_LL)	None	4.4 and 4.8 kN
Seat back rotational LL (SeatBack_LL)	None	61 kNm/deg

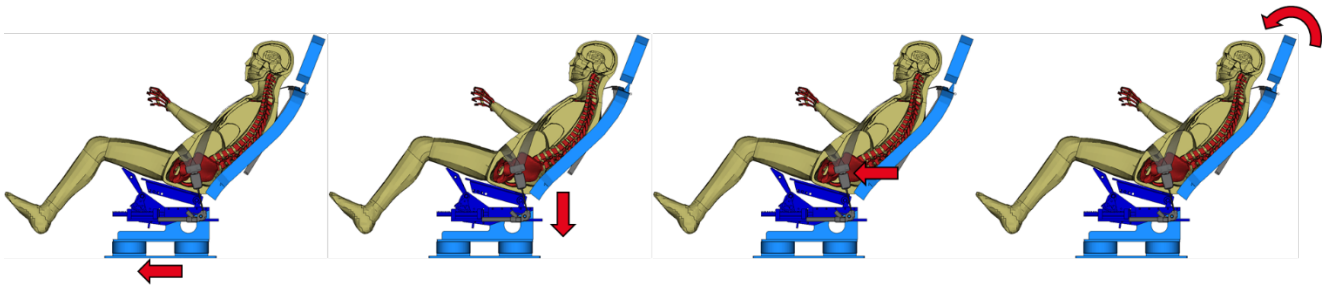

Fig. 5. Load limiting in the seat track (frontal direction), seat (vertical direction), lap belt (anchor and buckle sides) and seat back (rotational).

For the full factorial study, prescribed force-displacement relationships between the seat track and the floor and between the upper seat and the lower frame were used to implement load limiting for the semi-rigid seat model, Fig. 5 and Fig. *6*. The existing seat belt was modified by adding load limiters on both anchor and buckle sides: the force levels were chosen to equalise belt payout and load distribution for the two sides. Finally, a generic seat back was added with a prescribed rotational stiffness at the seat recliner point and to which the D-ring was mounted. No footwell was used.

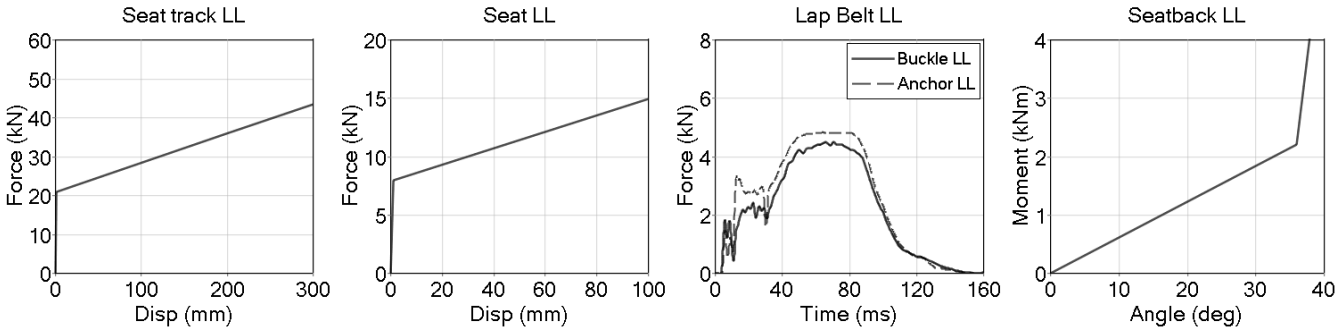

Fig. 6. Load limiting characteristics for seat track (frontal direction), seat (vertical direction), lap belt (anchor and buckle sides) and seat back (rotational).

Result parameters were the sum of resultant forces on the left and right iliac wings (ASIS), lumbar spine compression force (Fz) and lumbar spine flexion moment (My). Pelvis resultant forces were measured using cross section force measurements with respect to a local coordinate system in LS-Dyna, Fig. 7. Lumbar spine forces and moments were measured in the L1 to L5 vertebrae using cross section force-moment measurements with respect to a local coordinate system in the centre of each vertebra body (including ligaments). The maximum values from all five vertebrae were used as the result parameters.

Fig. 7. Cross section definitions (in red) for lumbar spine vertebra L1 (left) and pelvis ASIS (right). Intervertebral discs not shown for the lumbar spine.

III. RESULTS

Human Body Model Evaluation

The torso displacements predicted by the model correlated well with those of the PMHS tests, Fig. 8. The model predicted displacements of 439 mm for T1, 269 mm for T8, and 189 mm for T11. In the PMHS tests, displacements of 400–483 mm for T1, 252–315 mm for T8, and 193–241 mm for T11 were measured. The model predicted slightly smaller displacements for the lumbar spine, 133 mm for L1 and 130 mm for L3; the PMHS measurements were 168–184 mm and 142–184 mm, respectively, Fig. 8.

As Fig. 9 shows, in the PMHS tests pelvis displacements of 139–166 mm and peak rearward rotations of 3 deg were measured in the phase preceding rebound at 69 to 77 ms, after which the pelvis rotated forward. In the model, the increase of internal friction from 0.2 to 0.6 reduced the peak pelvis displacement, occurring at approximately 71 ms, from 144 mm to 130 mm. The increase in friction also reduced the pelvis rearward rotations at the time of pelvis rebound from 10 deg to 2 deg, correlating with the PMHS results.

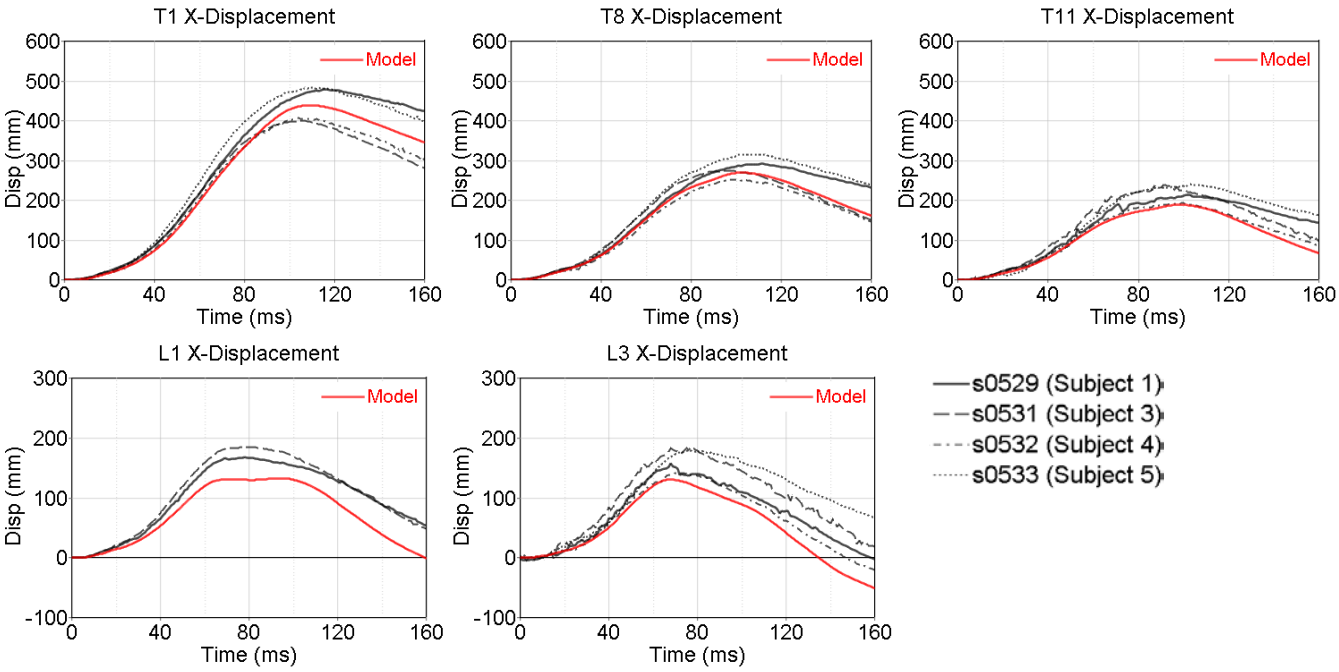

Fig. 8. Thoracic and lumbar spine x-displacements for the model and PMHS tests (see Table I).

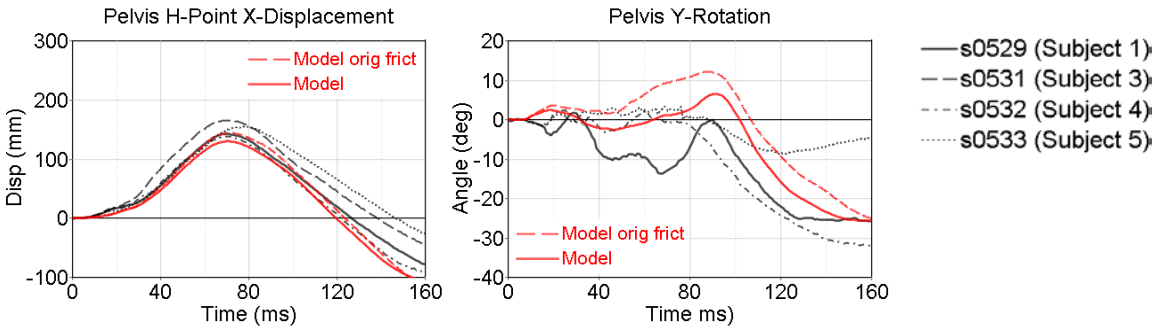

Fig. 9. Pelvis x-displacements and y-rotations for the model compared to PMHS tests according to Table I (positive rotation rearward). Pelvis rotation measurement failed in test s0531.

Lap belt forces at anchor and buckle sides matched the PMHS test measurements well, up to the time of pelvis fractures at 60 ms and 55 ms (s0529 and s0531) or submarining at 56 ms (s0533) [24], Fig. 10. Compared to the remaining s0532 test, peak lap belt forces on both sides were well predicted by the model. No submarining occurred with the HBM model.

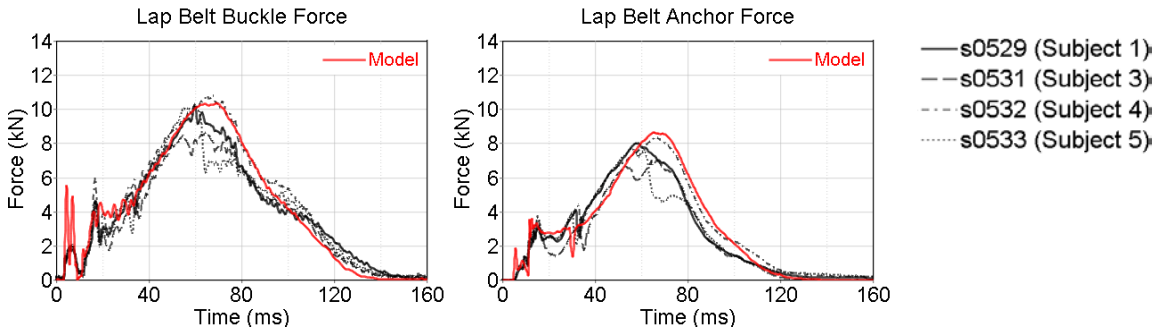

Fig. 10. Lap belt anchor and buckle forces for the model compared to PMHS tests according to Table I.

The highest CORA ratings (0.82–0.99) were obtained for the upper body displacements in T1, T8, and T11, and for the lap belt forces, Fig. 11 and Fig. 12. The lowest CORA rating (0.62) was obtained for the L3 displacement. Using the impact biofidelity requirements in ISO/TR 9790 [28] as a guideline, all responses were

rated either good or excellent, except for the L3 response, which was rated fair. A total CORA rating of 0.81 (good) was obtained for the whole model.

Num	ID	Response Name	No of tests
1	T1_dx	T1 X-Displacement	4
2	T8_dx	T8 X-Displacement	4
3	T11_dx	T11 X-Displacement	4
4	L1_dx	L1 X-Displacement	2
5	L3_dx	L3 X-Displacement	4
6	Pelv_dx	Pelvis X-Displacement	4
7	Pelv_ry	Pelvis Y-Rotation	3
8	Lap_f	Belt Force Lap Outboard (Anchor)	4
9	Buckle_f	Buckle Force	4

Fig. 11. CORA responses and number of tests for each response.

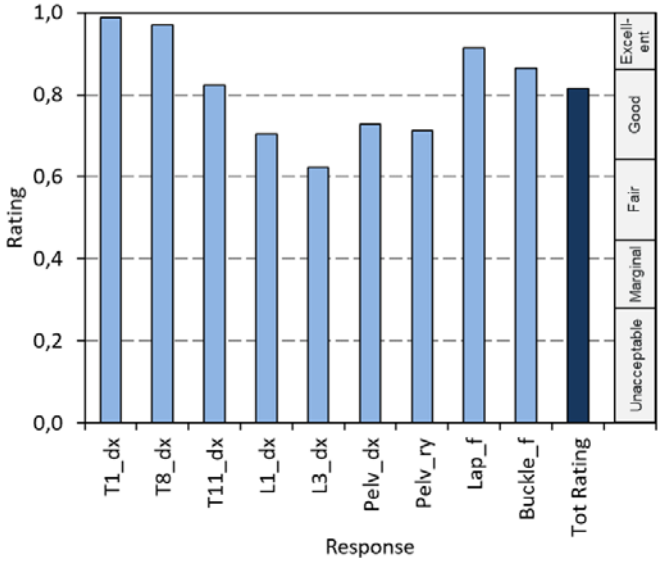

Fig. 12. CORA rating for each response and total SAFER HBM model (ISO/TR 9790 limits to the right)

Pelvis forces of 4.2 kN and 5.0 kN were obtained for left and right ASIS, respectively, Fig. 13. The maximum lumbar spine compression force in vertebra L1 was 3.9 kN and in L2 was 3.6 kN; both occurred at 64 ms. Maximum flexion moments of 88 Nm at 70 ms in L1 and 101 Nm at 74 ms in L2 were measured. While similar compression force levels were measured for all lumbar spine vertebrae, flexion moments decreased from L1 and L2 towards the pelvis and sacrum. Lumbar spine initial position and deformations at maximum loading and in the rebound phase are presented in Fig. 14.

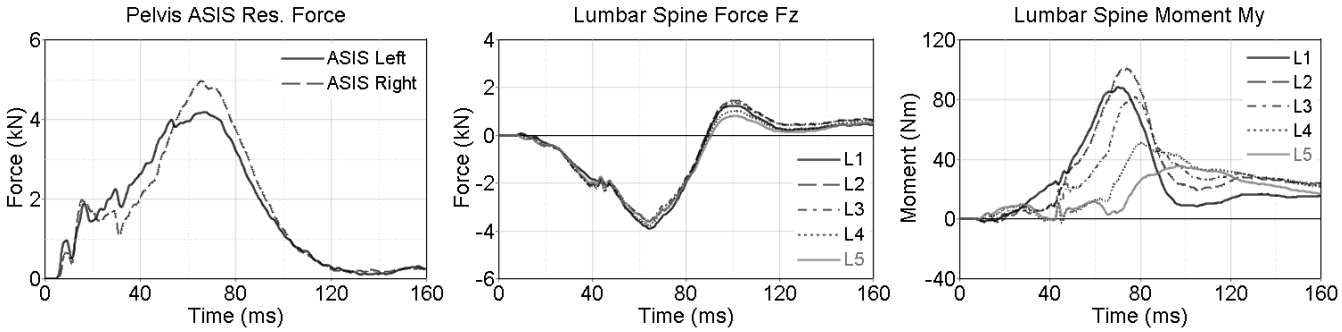

Fig. 13. SAFER HBM pelvis ASIS resultant forces and lumbar spine forces and moments for vertebra L1 to L5.

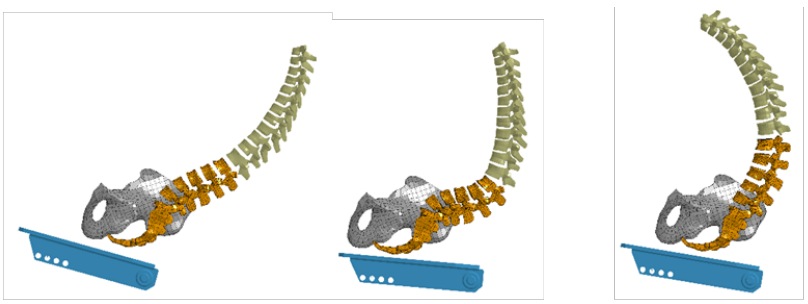

Fig. 14. Lumbar spine kinematics at 0 ms, 70 ms (maximum loading) and 100 ms (rebound phase).

Full Factorial Parameter Study

The main and interaction effects from the full factorial study are displayed as pareto charts showing the effects' absolute values. Only the factors seat track and seat load limiting had statistically significant results (α=0.05) on the lumbar spine loading, Fig. 15. Seat track load limiting resulted in average reductions of lumbar spine compression force and flexion moment of 1.1 kN and 27 Nm, respectively. Seat load limiting resulted in average reductions of 0.5 kN and 19 Nm, respectively. Although not significant, seat back load limiting resulted in small average reductions in the compression force and slightly increased average flexion moments (Table A2, Appendix).

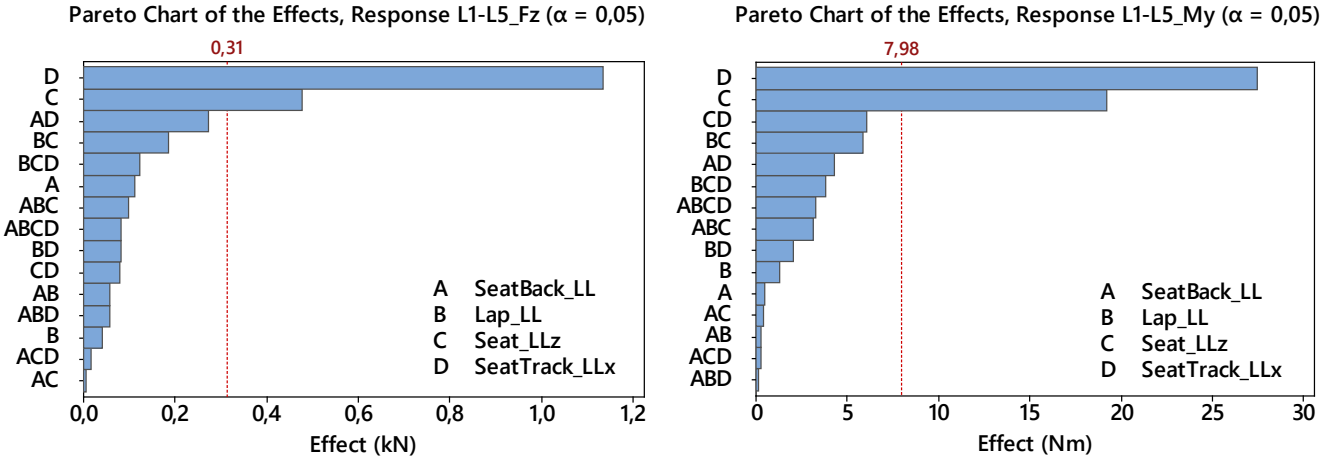

Fig. 15. Pareto charts of main and interaction effects for the lumbar spine compression force Fz (left) and flexion moment My (right). The dotted red reference lines show the limit value of the effect for a significance level of 0.05.

For the effect on pelvis ASIS total resultant force, seat track, seat and lap belt load limiting were statistically significant, Fig. 16. Seat track and lap load limiting reduced the pelvis force by an average of 2.3 and 2.2 kN, respectively, while seat load limiting reduced it by an average of 0.5 kN. A large interaction was observed between the factors seat track and lap load limiting – the effect of using lap load limiting was much smaller when the seat track load limiting was activated (Fig. A4, Appendix). On average, small increase of ASIS forces were obtained from seat back load limiting (Table A2, Appendix). A stable interaction between the lap belt and the pelvis was obtained for all load limiting factors (Fig. A7 and A8, Appendix).

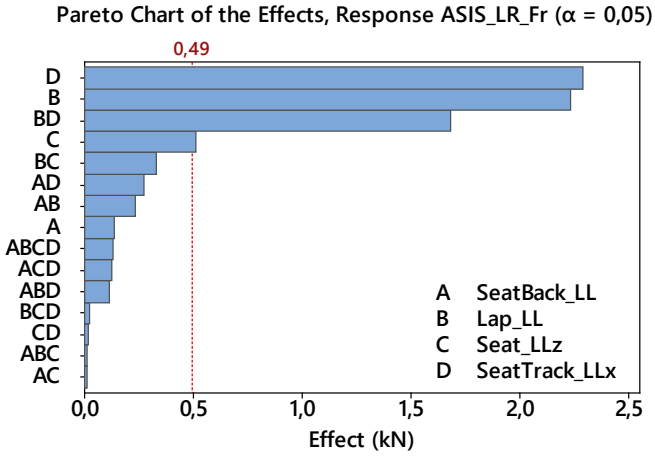

Fig. 16. Pareto charts of main and interaction effects for the pelvis (ASIS) total resultant force Fr. The dotted red reference line shows the limit value of the effect for a significance level of 0.05.

Largest reducing average effects on both lumbar spine and pelvis loading was obtained from the factors seat

track, seat, and lap belt load limiting. To illustrate the actual combined effect from using these three load limiters, the reduced loading on the lumbar spine and pelvis compared to not using load limiters, is shown in Fig. 17. The lumbar spine compression force was reduced from 4 to 2 kN and the flexion moment from 100 to 42 Nm. Peak compression force was measured in the L1 vertebra and in either the L1 or L2 vertebra for the flexion moment. The left ASIS force was reduced from 4.1 to 2.4 kN and the right ASIS force from 5.0 to 2.1 kN. Lap belt forces were reduced from 10.8 to 5.7 kN on the buckle side and from 9.3 to 4.4 kN on the anchor side. SAFER HBM kinematics with reduced lumbar spine deformations using load limiting are shown in Fig. 18 and time-history displacements in Fig. A6, Appendix. Seat track horizontal displacement of 207 mm and seat vertical displacement of 43 mm were obtained, due to load limiting (Fig. A5, Appendix).

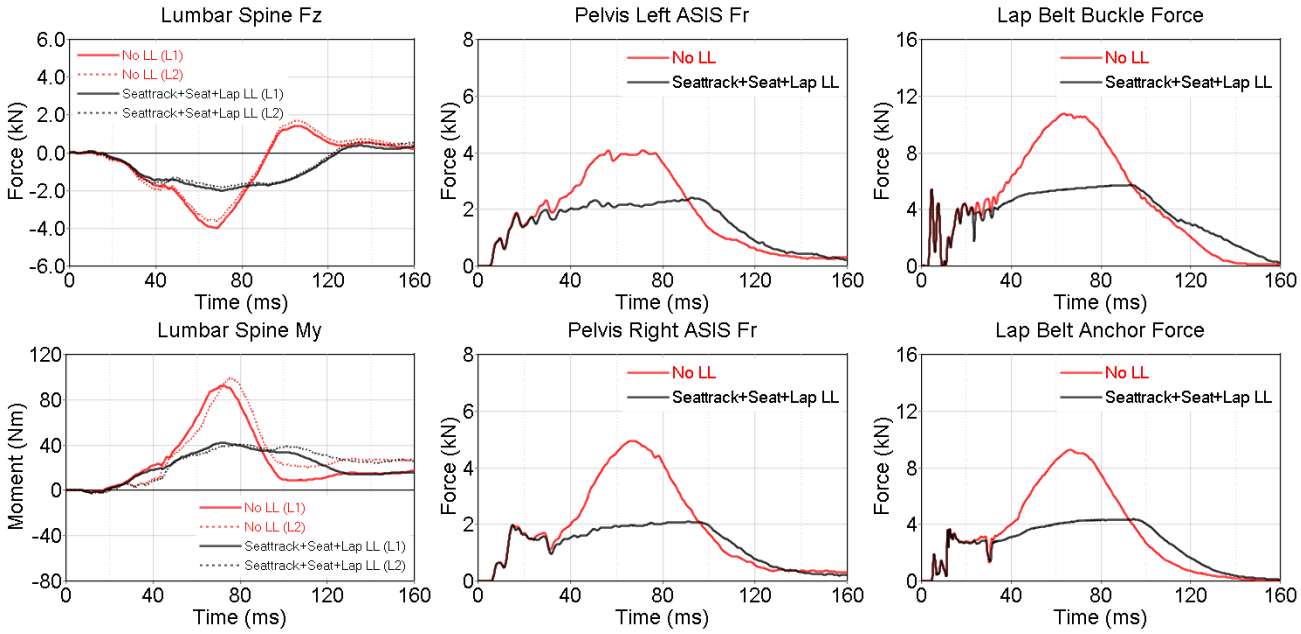

Fig. 17. Lumbar spine compression forces and flexion moments in L1 and L2 vertebrae, pelvis ASIS resultant forces left and right side, and lap belt buckle and anchor forces without load limiting (red) and the combination of seat track, seat and lap belt load limiting (black).

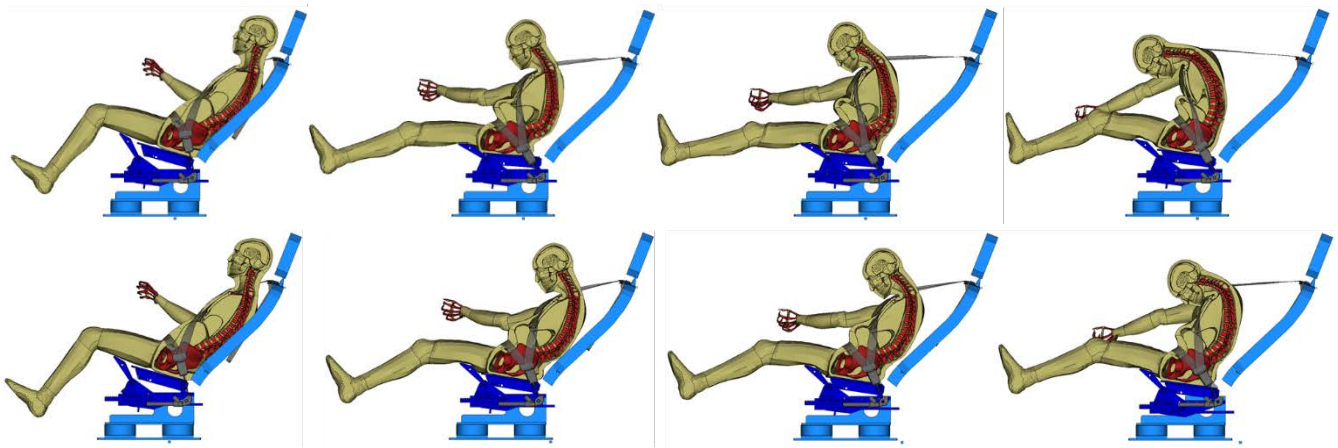

Fig. 18. SAFER HBM kinematics relative to the seat at 0, 70, 80 and 100 ms without load limiting (upper) and combined load limiting of the seat track, seat and lap belt (lower). For the combined load limiting, seat peak x-displacement of 207 mm was measured.

IV. Discussion

The kinematic response of the SAFER HBM was evaluated by four sled tests in frontal impacts with belted reclined average male PMHS. The evaluated model was used to investigate the effects of seat track, seat, seat back, and lap belt load limiting on the reduction of loading to the pelvis and lumbar spine.

Overall the HBM kinematics and belt forces correlated well with those of the PMHS tests, with a total CORA rating of 0.81. However, smaller x-displacements were predicted by the model than were observed in the PMHS lumbar spine region. There are several possible explanations for these differences. The HBM's shorter lumbar spine from the pelvis H-point to the L1 position (Fig. 4) promotes smaller displacements as it rotates around the pelvis during forward motion. Further, the PMHS pelvis fractures, which were not considered in the HBM, increased displacements of the lumbar spine. Finally, submarining was observed for one of the PMHS tests but not for the HBM. To account for submarining in the HBM, personalized morphing of the pelvic bone and surrounding adipose tissue geometries for refined interaction to the lap belt might be needed in future studies.

In two of the PMHS tests, right pelvis ASIS fractures were obtained at 55–60 ms with a lap belt force of 6.6–7.8 kN. In the HBM, in the time window with the same belt force, forces of 3.6–4.4 kN were measured at the right ASIS. This simple comparison provides an initial estimation for a critical pelvis (ASIS) force; more research is needed to derive a more precise critical force level for pelvis iliac wings loaded by seat belts. In this future research, also the pelvic to lap belt relative position and angle should be considered, in addition to the belt force, as this has been shown to affect the risk of pelvis fractures in [14].

For the HBM lumbar spine, peak compression forces were measured 7 ms before peak pelvis displacement while peak flexion moments were measured at the start of or during the rebound of the pelvis. Thus, for vertebrae L1 and L2, the peak flexion moment occurred 6–10 ms later than the peak compression force. As the injurious loading is likely a combination of both compression force and flexion moment, it cannot be determined which is the more highly loaded vertebra of the two. However, the area of peak loading matches other studies, in which most of the thoracolumbar fractures in frontal impacts occurred in the transition between the thoracic and lumbar spine [6,9,29]. Without considering the flexion moment contribution, the highest compression force of 3.9 kN was measured in the L1 vertebra which is within the 3.7–4.5 kN tolerance level range at 50% risk of injury as proposed in [30,31]. The complex HBM kinematics of the lumbar spine indicate that there is a need for more studies to derive lumbar spine tolerance limits in combined compression and flexion loading.

The evaluated model was used in the parameter study with the footwell removed in order to anticipate its lack in future vehicles. As a result, the effects in the parameter study were derived from a model which differed from the previously evaluated model with PMHS tests, but only slightly. Without a footwell, the upper legs interacted more with the seat submarining pan and the lap belt anchor force increased (from 8.7 to 9.3 kN), as did buckle force (from 10.4 to 10.8 kN). For the HBM, the pelvis displacements increased from 130 to 140 mm and the rotations rearward decreased from 6.5 deg to 1.7 deg. The pelvis ASIS force remained 4.2 kN on the left side and decreased from 5.0 to 4.9 kN on the right side, while lumbar spine L1 compression force increased from 3.9 kN to 4.1 kN and the L1 flexion moment increased from 88 to 93 Nm. The risk of submarining did not increase.

The primary loading on the lumbar spine was determined by the structure supporting the pelvis, as indicated by the large effects from load limiting of the seat and seat track. The results also indicate that the seat load limiting has a larger effect on flexion moment than on compression forces. The loading on the lumbar spine was measured using force and moment on the most loaded vertebrae (L1 to L5). Treating force and moment as independent parameters does not account for the fact that the risk of injury is a combination of the two. However, for all load limiting combinations the maximum loading was obtained in either the L1 or L2 vertebra.

For pelvis ASIS, the primary loading was from the lap belt. Lap belt load limiting thus reduces the pelvis loading directly, while seat track load limiting reduces it indirectly through decreased lap belt forces. This relationship was also visible in the large interaction effect between seat track and lap load limiting – the additional effect from lap load limiting was small, due to the reduced lap belt forces from seat track load limiting.

For the selected example of combined load limiting in the seat track, seat, and lap belt, the lumbar spine compression force was reduced to 2 kN, less than the current injury threshold of 3.7-4.5 kN [30,31], and the flexion moment was reduced to 42 Nm, less than the threshold of 174 Nm for loading in combined anterior shear-flexion [32]. The right pelvis ASIS force was reduced by 43% from 3.7 kN (above the estimated injurious force from the HBM in this study) to 2.1 kN (below). A similar reduction was achieved on the left side. Lap belt forces were reduced to 5.7 kN in the buckle and to 4.4 kN on the anchor side. The reduced risk of pelvis fractures using lap belt load limiting has been shown in earlier studies: fractures were obtained for lap belt loads of 6.2–6.8 kN [13] but no fractures occurred when loads were reduced to 5 kN by lap belt load limiting [14].

Several limitations exist in the parameter study. No sensitivity analysis or optimisation of the load limiting values and characteristics was carried out, although the authors believe they have made plausible choices. The quantification of load limiting effects might be affected by different choices. As the semi-rigid seat is heavier than a typical vehicle seat, the load limiting characteristics was adjusted accordingly. Also, the effect of the seat load limiting in the vertical direction may have been overestimated, because in this direction the semi-rigid seat is estimated stiffer than most production seats. The consequence from this may be that the lumbar spine loading increase slightly from using lap belt load limiting but the reducing effect on ASIS loading remains (Fig. A2-A3, Appendix). The load limiting levels for the seat and lap belt were defined in a pre-study in which the available displacement range in a vehicle was considered. Maximum load limiting displacements of 220 mm in the seat track, 90 mm in the seat vertical direction and lap belt payout of 80-100 mm (Fig. A5, Appendix) were all are estimated feasible to implement in a vehicle. However, larger occupants, posture, seat stiffness and potential interaction to kneebolster are factors which may influence the lap belt load limiting levels and needs to be considered in future studies.

The results from this study give important insights into the design of restraint systems for the protection of occupants in vehicles that allow for reclined postures and seated positions away from frontal airbags and knee bolster. Such restraint systems are expected to be seat-integrated to allow for flexible arrangements of the seat, seat cushion, and seat back [33], including reclined postures, which put occupants at increased risk of submarining. This risk can be mitigated with lap belt pretensioning and restraints such as the pelvis restraint cushion [12,26,34]. Once submarining is mitigated, design principles as in this study, but potentially also the pelvis restraint cushion, can be used to limit pelvis and lumbar loading. Additionally, it is expected that also overall loading to the upper body and head can be reduced as the peak forces decrease with longer stopping distance. Further, seat track and lap belt load limiting can probably be adjusted to reduce pelvis and lumbar spine loading for upright occupants as well. Finally, while seat back load limiting played only a small role in reducing lower body loading, it might well play a larger role in reducing loading on the head, neck, thoracic spine and chest. This needs to be investigated in future studies.

V. CONCLUSIONS

The SAFER HBM sled model was shown to correlate well to PMHS tests for the front reclined scenario with respect to kinematics and boundary conditions. Seat track and seat load limiting were most effective at reducing lumbar spine loading. Seat track and lap belt load limiting were most effective at reducing pelvis loading, while seat back load limiting affected pelvis and lumbar spine loading only marginally.

VI. ACKNOWLEDGEMENT

The work was carried out as part of the OSCCAR project, which has received funding from the European Union’s Horizon 2020 Research and Innovation Programme under Grant Agreement No 768947. The authors would like to thank Kristina Mayberry for language revisions.

VII. REFERENCES

[1] Filatov, A., Scanlon, J., Bruno, A., Danthurthi, S. (2019) Effects of Innovation in Automated Vehicles on Occupant Compartment Designs, Evaluation, and Safety: A Review of Public Marketing, Literature, and Standards. *SAE Technical Paper 2019-01-1223*.

[2] Östling, M., Larsson, A. (2019) Occupant Activities and Sitting Positions in Automated Vehicles in China and Sweden. *Proceedings of Conference for the Enhancement of Safety Vehicles, 2019*. Paper Number 19-0083, Eindhoven, Netherlands.

[3] Jorlöv, S., Bohman, K., Larsson, A. (2017) Seating Positions and Activities in Highly Automated Cars - A Qualitative Study of Future Automated Driving Scenarios. *Proceedings of the IRCOBI Conference*, 2017, Antwerp, Belgium.

[4] Poplin, G.S., McMurry, T.L., et al. (2015) Nature and etiology of hollow-organ abdominal injuries in frontal crashes. Accident Analysis and Prevention, 78: pp.51-57.

[5] Jakobsson, L., Bergman, T., Johansson, L. (2006) Identifying Thoracic and Lumbar Spinal Injuries in Car

Accidents. *Proceedings of IRCOBI Conference*, 2006, Madrid, Spain.
[6] Pintar, F.A., Yoganandan, N., Maiman, D.J., Scarboro, M., Rudd, R.W. (2012) Thoracolumbar Spine Fractures in Frontal Impact Crashes. *Proceedings of Association of the Advancement of Automotive Medicine*, 2012. Vol 56.
[7] Forman, J., Poplin, G.S., et al. (2019) Automobile injury trends in the contemporary fleet: Belted occupants in frontal collisions. *Traffic Injury Prevention*. Vol 20(6):607-612.
[8] Adolph, T., Wisch, M., et al. (2013) Analyses of Thoracic and Lumbar Spine Injuries in Frontal Impacts. *Proceedings of the IRCOBI Conference*, 2013, Gothenburg, Sweden.
[9] Shaikh, J., Thathia, H., Lubbe, N. (2020) Lumbar Spine Injuries in Motor Vehicle Crashes. *Proceedings of IRCOBI Asia Conference*, 2020, Beijing, China (Accepted).
[10] Jones, D.A., Gaewsky, J.P., et al. (2016) Lumbar vertebrae fracture injury risk in finite element reconstruction of CIREN and NASS frontal motor vehicle crashes. *Traffic Injury Prevention*, 17:sup1: pp.109-115.
[11] Luet, C., Trosseille, X., Drazétic, P., Potier, P., Vallancien, G. (2012) Kinematics and Dynamics of the Pelvis in the Process of Submarining using PMHS Sled Tests. *Stapp Car Crash Journal*, Vol 56: pp.411-442.
[12] Shaw, G., Lessley, D., et al. (2018) Pelvic restraint cushion sled test evaluation of pelvic forward motion. *Traffic Injury Prevention*, Vol 19:3, pp.250-255.
[13] Uriot, J., Potier, P., et al. (2015) Comparison of HII, HIII and THOR dummy responses with respect to PMHS sled tests. *Proceedings of IRCOBI Conference*, 2015, Lyon, France.
[14] Uriot, J., Potier, P., et al. (2015) Reference PMHS Sled Tests to Assess Submarining. *Stapp Car Crash Journal*. Vol 59.
[15] Iwamoto, M., Kisanuki, Y., et al. (2002) Development of a Finite Element Model of the Total Human Model for Safety (THUMS) and Application to Injury Reconstruction. *Proceedings of IRCOBI Conference*, 2002, Munich, Germany.
[16] Iraeus, J., Pipkorn, B. (2019) Development and Validation of a Generic Finite Element Ribcage to be used for Strain based Fracture Prediction. *Proceedings of the IRCOBI Conference*, 2019, Florence, Italy.
[17] Afewerki, H. (2016) Biofidelity Evaluation of Thoracolumbar Spine Model in THUMS, *Master's thesis in Biomedical Engineering*. Chalmers University of Technology, Sweden.
[18] Östh, J., Bohman, K., Jakobsson, L. (2020) Evaluation of Kinematics and Restraint Interaction when Repositioning a Driver from a Reclined to Upright Position Prior to Frontal Impact using Active Human Body Model Simulations. *Proceedings of the IRCOBI Conference*, 2020, Munich, Germany.
[19] Pipkorn, B., Iraeus, J., Björklund, M., Bunketorp, O., Jakobsson, L. (2019) Multi-Scale Validation of a Rib Fracture Prediction Method for Human Body Models. *Proceedings of the IRCOBI Conference*, 2019, Florence, Italy.
[20] Gepner, B.D., D. Draper, et al. (2019) Comparison of Human Body Models in Frontal Crashes with Reclined Seatback. *Proceedings of the IRCOBI Conference*, 2019, Florence, Italy.
[21] Richardson, R., Donlon, J.P., et al. (2019) Test methology for evaluating the reclined seating environment with human surrogates. *Proceedings of Conference for the Enhancement of Safety Vehicles,* 2019, Eindhoven, Netherlands.
[22] Hallquist, J.O. (2016) LS-DYNA Theoretical Manual, May 2006. Livermore Software Technology Corporation, USA.
[23] Minitab Inc. (2017) Minitab Statistical Software, Release 17 for Windows. State College, Pennsylvania, USA.
[24] Richardson, R., Jayathirtha, M., et al. (2020) Pelvis Kinematics and Injuries of Reclined Occupants in Frontal Impact. *Proceedings of the IRCOBI Conference*, 2020, Munich, Germany (Submitted).
[25] Richardson, R., Jayathirtha, M., et al. (2020) Thoracolumbar Spine Kinematics and Injuries in Frontal Impacts with Reclined Occupants. *Proceedings of Association of the Advancement of Automotive Medicine,* 2020, Portland, Oregon, USA (Submitted).
[26] Östling, M., Sunnevång, C., Svensson, C., Kock, H.-O. (2017) Potential future seating positions and the impact on injury risks in a Learning Intelligent Vehicle (LIV). How to avoid submarining in a reclined seating position in a frontal crash. *Conference: 11. VDI-Tagung Fahrzeugsicherheit*, 2017, Berlin, Germany.
[27] Kerrigan, J.R. "Positioning Data for Human Body Models in Reclined Seating, March 16, 2020", https://virginia.app.box.com/s/pm1g83555o7kiqie0xlpnyjp51kmg363. Center for Applied Biomechanics, University of Virginia, USA [Accessed March 30, 2020].
[28] Thunert, C. (2017) CORAplus Release 4.0.4 User's Manual, May 2017. PDB–Partnership for Dummy Technology and Biomechanics, www.pdb-org.com, Germany.

[29] Jakobsson, L., Björklund, M., Westerlund, A. (2016) Thoracolumbar Spine Injuries in Car Crashes. *Proceedings of the IRCOBI Conference*, 2016, Malaga, Spain.
[30] Stemper, B.D., Chirvi, S., et al. (2017) Biomechanical Tolerance of Whole Lumbar Spines in Straightened Posture Subjected to Axial Acceleration. *Journal of Orthopaedic Research*, 36(6).
[31] Yoganandan, N., Arun, M.W.J., Stemper, B.D., Pintar, F.A., Maiman, D.J. (2013) Biomechanics of Human Thoracolumbar Spinal Column Trauma from Vertical Impact Loading. *Annals of Advances in Automotive Medicine*. Vol 57: pp.155-66.
[32] Belwadi, A. and Yang, K.H. (2008) Cadaveric lumbar spine responses to flexion with and without anterior shear displacement. *Proceedings of IRCOBI Conference*, 2008, Bern, Switzerland.
[33] Velavan, S.S., Huf, A. (2018) Development of Occupant Restraint Systems for Future Seating Positions in Fully or Semi Autonomous Vehicles, *Society of Automotive Engineers India, F2018/F2018-APS-056*.
[34] Mroz, K., Pipkorn, B., Kim, H.J., and Crandall, J. (2017) Investigation of Pelvis Kinematics for Various Lap Belt Positions and an Inflatable Pelvis Restraint Cushion Using a Human Body Model of a Female Occupant. *Proceedings of Conference for the Enhancement of Safety Vehicles,* 2017, Detroit, Michigan, United States.

VIII. APPENDIX

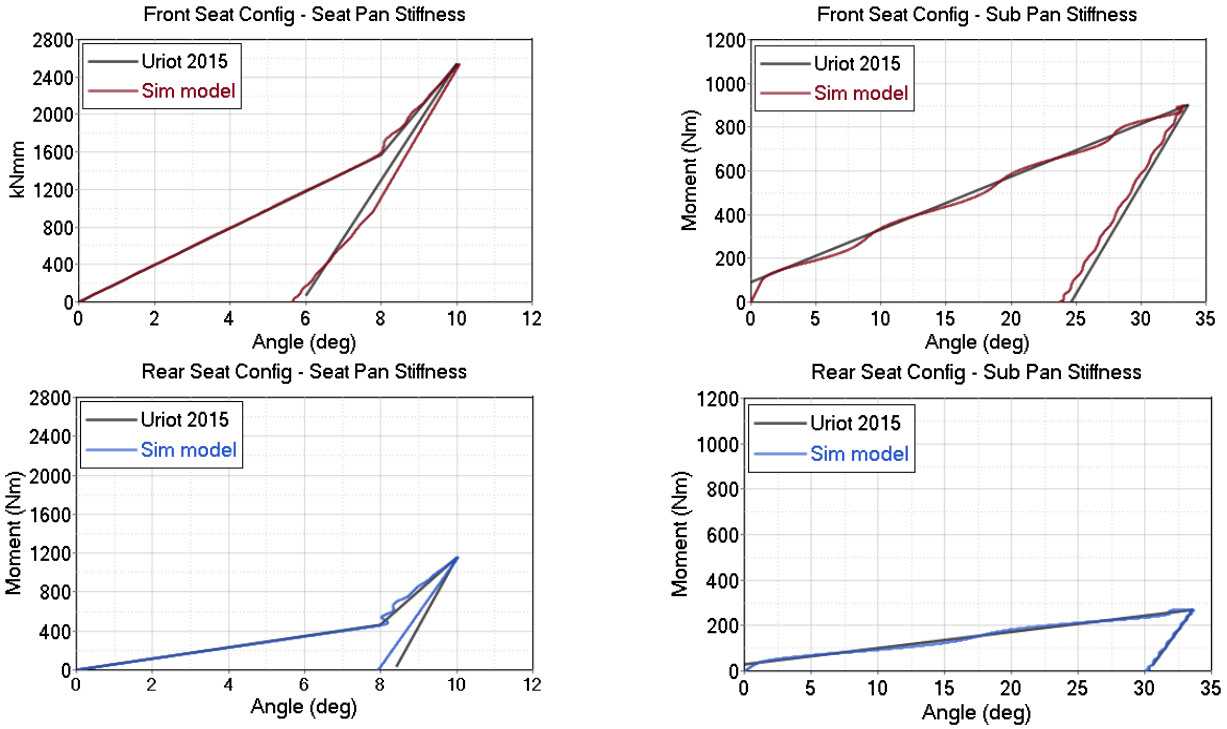

Fig. A1. Validation of the semi-rigid seat model. Seat pan and sub pan rotational stiffness characteristics of the model compared to reference data in [14]. Seat pan side springs stiffness 128 N/mm (front config) and 37 N/mm (rear config). Sub pan spring stiffness 123 N/mm (front config) and 36.7 N/mm (rear config). Seat pan centre spring stiffness 350 N/mm.

TABLE AI
TWO-LEVEL FULL FACTORIAL STUDY WITH FOUR FACTORS

Run	SeatBack_LL (A)	Lap_LL (B)	Seat_LLz (C)	SeatTrack_LLx (D)
1	0	0	0	0
2	1	0	0	0
3	0	1	0	0
4	1	1	0	0
5	0	0	1	0
6	1	0	1	0
7	0	1	1	0
8	1	1	1	0
9	0	0	0	1
10	1	0	0	1
11	0	1	0	1
12	1	1	0	1
13	0	0	1	1
14	1	0	1	1
15	0	1	1	1
16	1	1	1	1

TABLE AII
MAIN, TWO- AND THREE-WAY INTERACTION EFFECTS. FOR THE MAIN EFFECTS (A TO D), NEGATIVE EFFECTS REDUCE THE RESPONSE. FOR NEGATIVE TWO-WAY INTERACTION EFFECTS (FOR EXAMPLE AB), INCREASE OF THE FIRST FACTOR (A) WILL DECREASE THE SIGNIFICANCE EFFECT OF THE SECOND FACTOR (B).

Factor	Factor Alias	L1-L5_Fz (kN)	L1-L5_My (Nm)	ASIS_LR_Fr (kN)
SeatBack_LL	A	-0,11	0,5	0,13
Lap_LL	B	0,04	1,3	-2,23
Seat_LLz	C	-0,48	-19,2	-0,51
SeatTrack_LLx	D	-1,14	-27,5	-2,29
*SeatBack_LL*Lap_LL*	AB	-0,06	0,3	-0,23
*SeatBack_LL*Seat_LLz*	AC	-0,01	0,4	0,01
*SeatBack_LL*SeatTrack_LLx*	AD	0,27	4,3	-0,27
*Lap_LL*Seat_LLz*	BC	0,18	5,9	0,33
*Lap_LL*SeatTrack_LLx*	BD	-0,08	-2,1	1,68
*Seat_LLz*SeatTrack_LLx*	CD	0,08	6,0	-0,02
*SeatBack_LL*Lap_LL*Seat_LLz*	ABC	-0,10	-3,1	-0,01
*SeatBack_LL*Lap_LL*SeatTrack_LLx*	ABD	0,06	0,2	0,11
*SeatBack_LL*Seat_LLz*SeatTrack_LLx*	ACD	0,02	0,3	0,13
*Lap_LL*Seat_LLz*SeatTrack_LLx*	BCD	-0,12	-3,9	0,02
*SeatBack_LL*Lap_LL*Seat_LLz*SeatTrack_LLx*	ABCD	0,08	3,2	-0,13

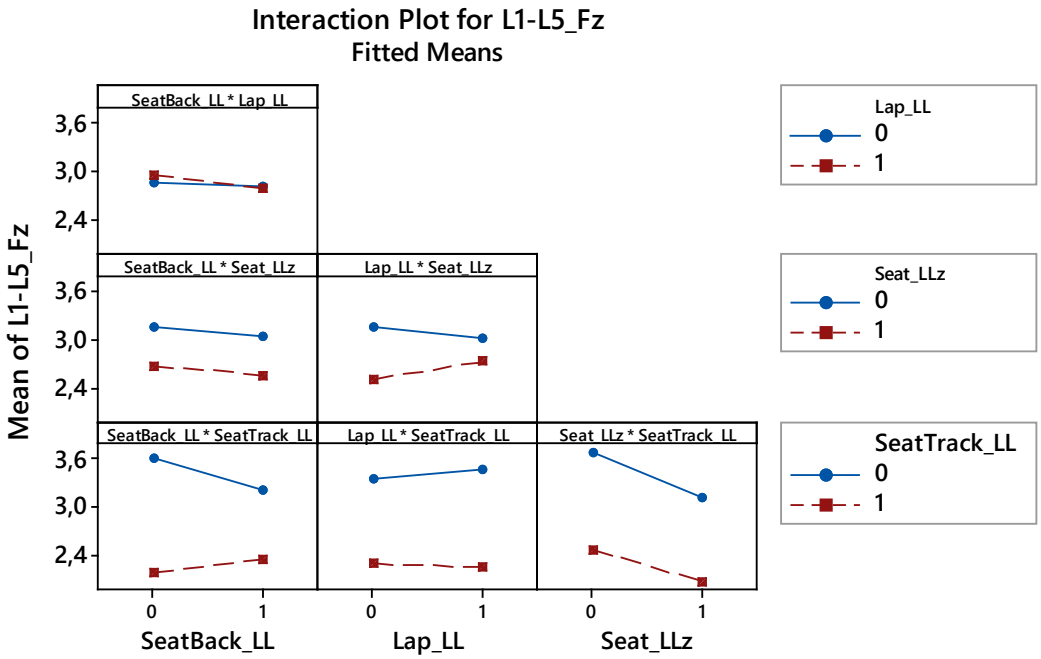

Fig. A2. Two-way interaction plots for lumbar spine vertebra max L1-L5 compression force Fz.

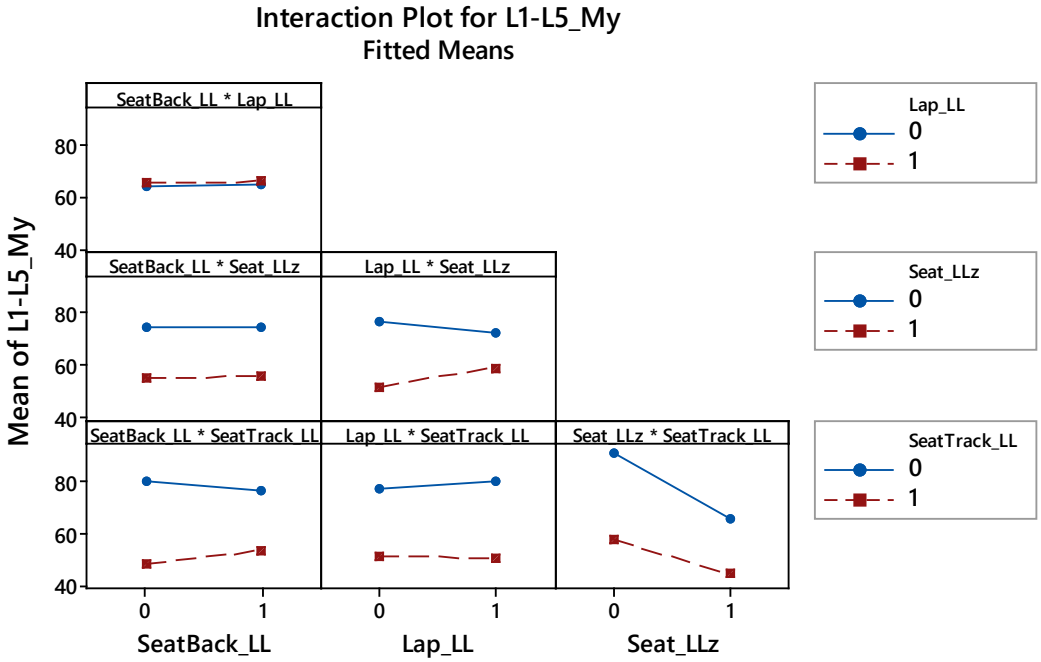

Fig. A3. Two-way interaction plots for lumbar spine max L1-L5 flexion moment My.

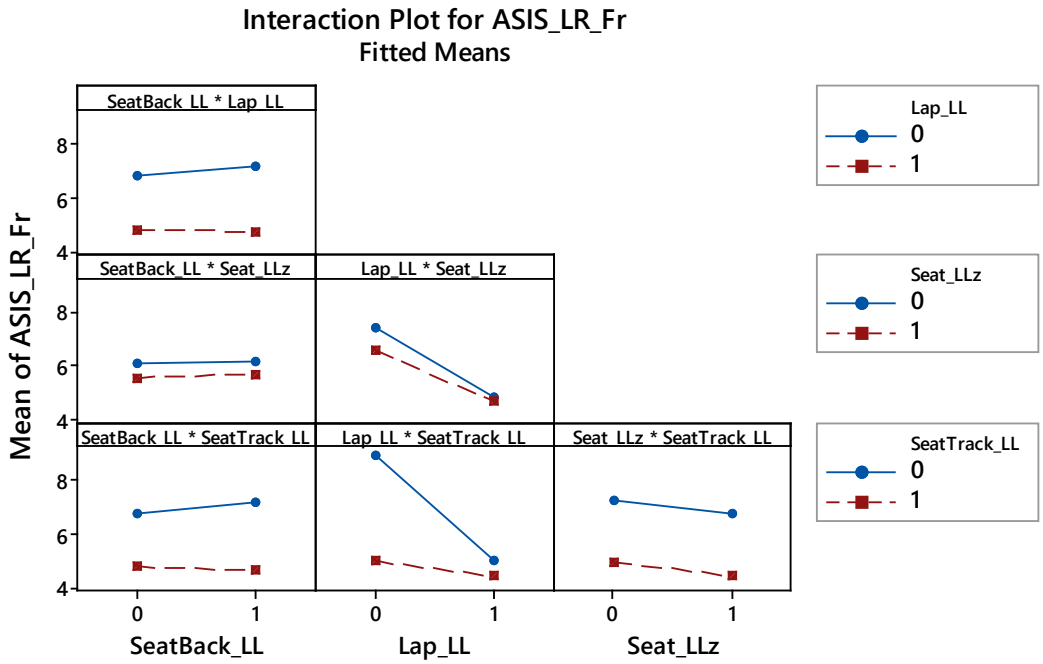

Fig. A4. Two-way interaction plots for pelvis ASIS total resultant force.

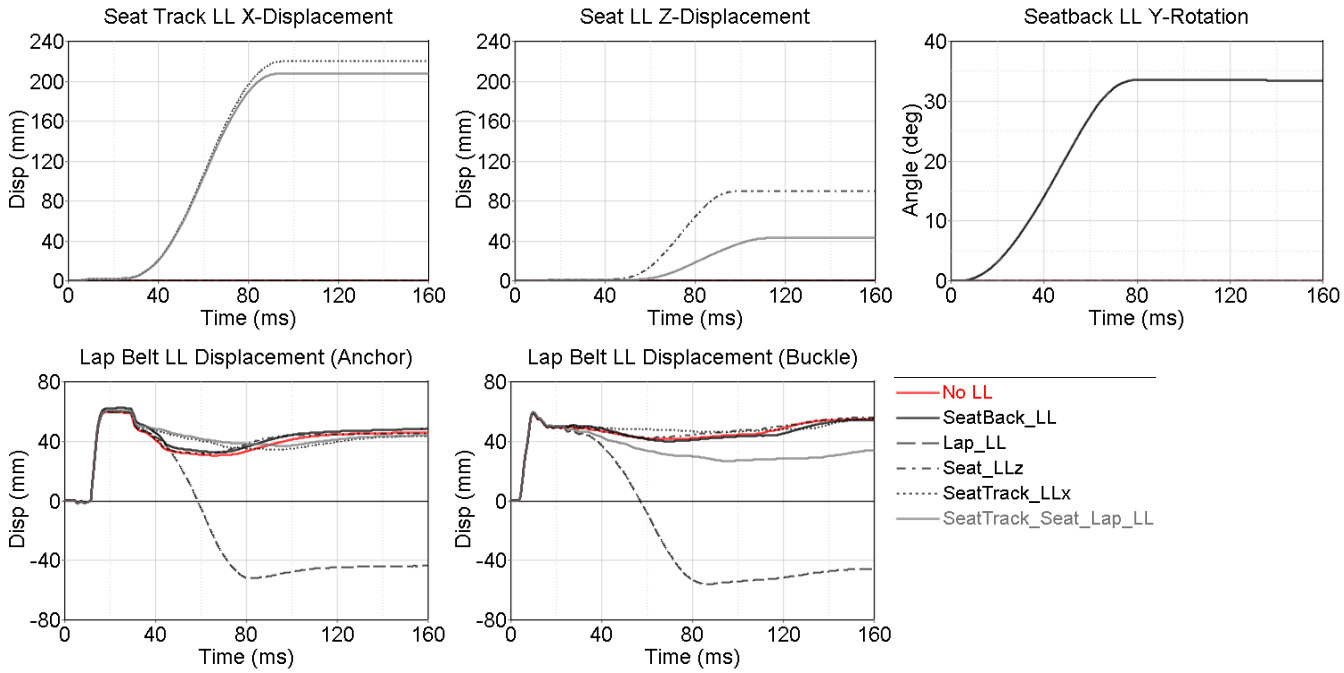

Fig. A5. Load limiting displacements for the seat track (x), seat (z) and seat back (y-rotation) together with the lap belt anchor and buckle pretensioning and load limiting displacements.

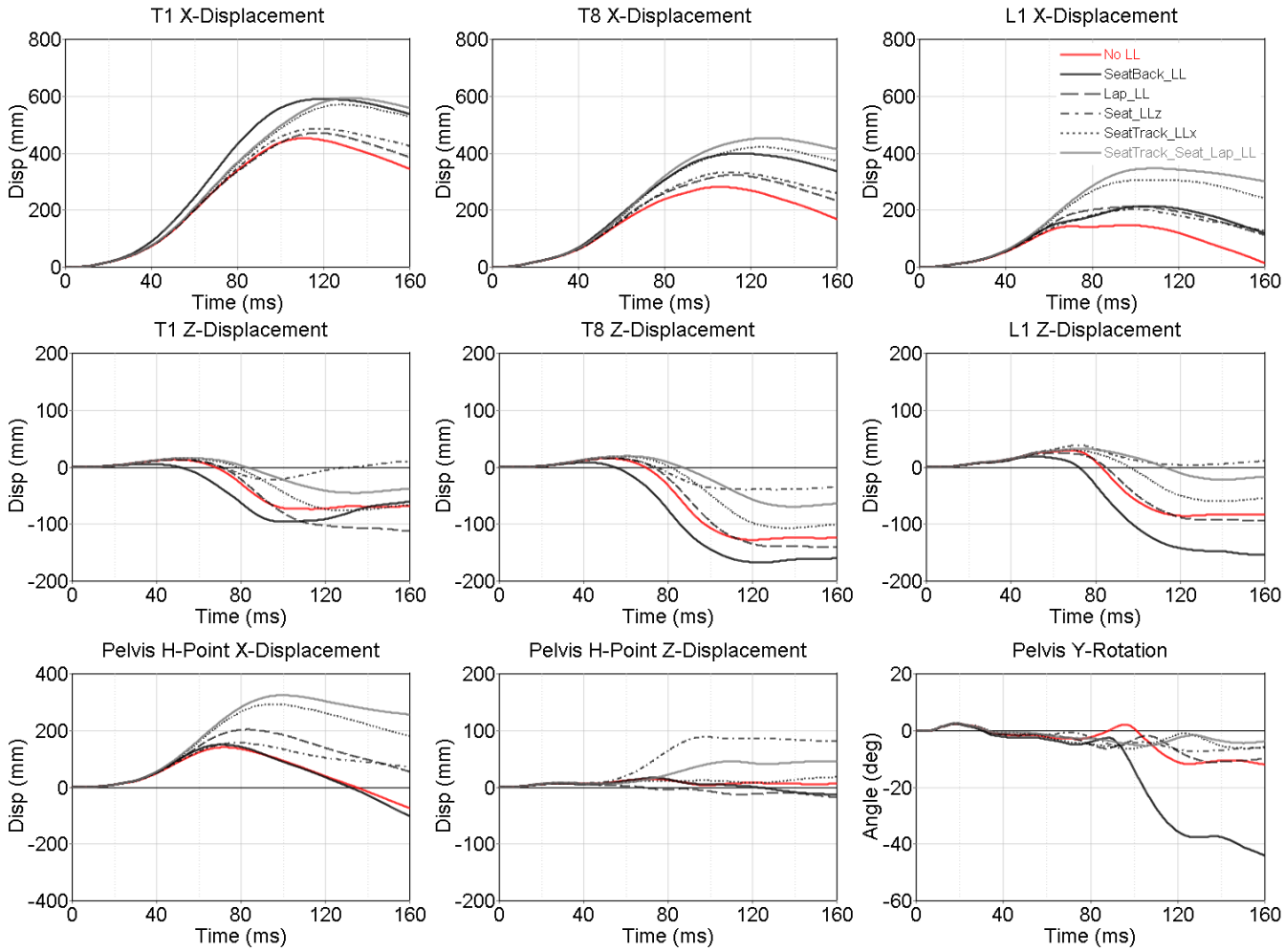

Fig. A6. SAFER HBM x- and z-displacements for the T1, T8, L1 and pelvis together with pelvis rotations. Single load limiting in the seatback (run 2 in Table AI), lap belt (3), seat (5), seat track (9) and the combination of seat track, seat and lap LL (15) are compared to no load limiting (1). Positive directions defined as forward for x-displacements and downwards for z-displacements. For positive angles, the pelvis is rotating rearwards.

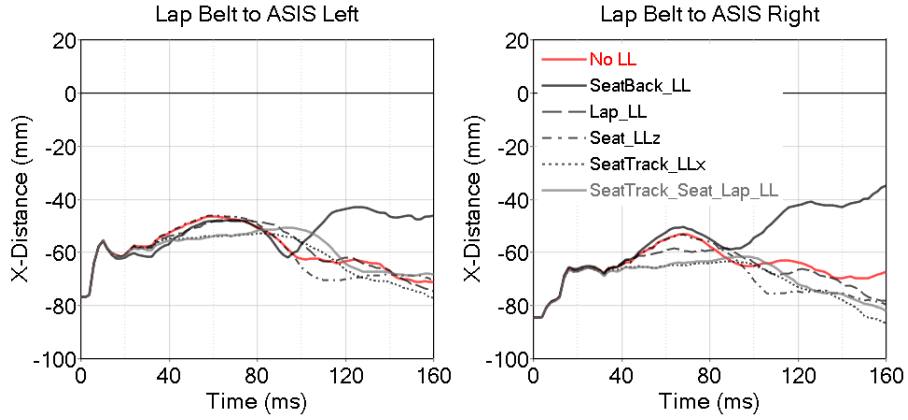

Fig. A7. Submarining distance at left and right ASIS. Submarining distance is defined as the ASIS x-position relative to the lap belt midpoint x-position [34]. Positive values of the submarining distance indicate that the ASIS is forward of the lap belt and thus the occurrence of submarining.

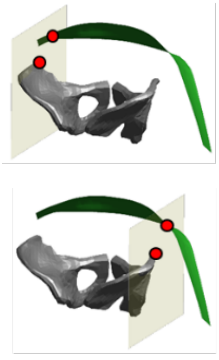

Fig. A8. Submarining distance measurement points on pelvis and lap belt at left and right ASIS sagittal planes [34].